

Heat Exchange and Flow Characteristics of a cooled EGR Module Evaluated in Automotive Operating Conditions

Adrian Irimescu, Simona Silvia Merola, Vasco Zollo, Raffaele De Marinis, Bianca Maria Vaglieco

Abstract—Compression ignition engines are an essential part of automotive transportation and even marginal improvements can bring significant benefits in terms of costs and environmental impact. Exhaust gas recirculation (EGR) is used on an extensive scale for these power units, and monitoring their performance continuously would ensure improved procedures for ensuring longer lifetime and better efficiency. Within this context, the current work evaluated the heat transfer performance of a cooled EGR module in view of developing a dedicated sensor. This device should provide enough information on heat exchange and flow performance of the recirculation unit, while being able to integrate the acquired information within the vehicle communication network. Apart from the minimal requirement of identifying failures, the new component goes beyond current virtual-sensor based approaches and will ensure better efficiency of EGR valves and more precise maintenance intervals.

Keywords—EGR module, compression ignition engines, heat transfer, flow characteristics

I. Introduction

Internal combustion engines are continuously being improved [1], even for marginal gains, and compression ignition (CI) units hold a significant share in the automotive transport sector [2]. They deliver high efficiency and can ensure reduced environmental impact, with the latter featuring even more possibility of reduction when using alternative fuels [3]. High adaptability to alternative combustion modes can provide further enhanced efficiency and emissions characteristics [4] and optimization of different components [5] ensures reliable operation with a wide range of fuel specifications.

One specific aspect of CI units is the use of cooled exhaust gas recirculation (EGR) for controlling nitrogen oxide emission (NO_x) [6], [7]. This technology combines a recirculation valve and a heat exchanger (usually gas-liquid). The efficiency of EGR modules tends to degrade over time, mainly due to fouling phenomena [8], [9]. Evidently, this affects the gas side, with condensation being an important driver.

These mechanisms can lead to plugging of gas passages, significantly affecting module performance [10], [11]. Given these problems, the ability to continuously monitor the performance of cooling effectiveness would be an important advantage. It could ensure better performance throughout the lifetime of the product, not to mention significant benefits with respect to fuel consumption and emissions. Usually this task is partially performed based on a ‘virtual sensor’ approach [12], [13], [14], [15], that determines information on the recirculated gas through post-processing of data acquired indirectly (e.g. based on recorded air flow, intake manifold temperature, pressure etc. and comparing the data with expected values for certain EGR valve lift values) and application of fast running models [16], [17]. This straightforward and standardized approach is aimed at detecting failures, but cannot evaluate whether the module is operating at its rated flow and heat transfer parameters. The main reason is that the measurement chain features relatively low accuracy and thus actual flow values can only be determined with high error levels. Relatively high complexity of fluid flow (usually ranging from laminar to transitory) and heat transfer phenomena means that most development is aimed at the gas side. As the previous analysis showed, fouling and condensation mechanisms further emphasize this need.

Within this context, the present work looked at the performance of an automotive EGR module. Its efficiency was determined based on flow and temperature measurements, for the gas and liquid sides. The valve-heat exchanger module was fitted at the exhaust of a CI engine, setup that ensured a wide range of operating conditions. Calculated heat transfer coefficients were compared to values obtained by applying empirical *Nu-Re* type correlations. This will allow development of a hardware in the loop setup aimed at testing the newly developed sensor in the widest possible range of situations.

II. Experimental setup and procedure

The EGR module that was investigated is generally fitted to Diesel engines with 3 and 4 cylinders inline configuration, displacement of 1.2 to 1.6 litres and 55 to 77 kW rated power. By analyzing general recirculation maps (i.e. percentages listed in tables organized based on engine speed and load), it was concluded that EGR is mostly used in conditions with reduced brake mean effective pressure (BMEP), relatively low engine speed and thus practically little or no boost. With these targets in mind, an aspirated Diesel unit was chosen, and the

Adrian Irimescu*, Simona Silvia Merola, Bianca Maria Vaglieco
Istituto Motori – CNR
Via G. Marconi 4, 80125 Napoli, Italy

Vasco Zollo, Raffaele De Marinis
Demax SRL
Boscofangone ASI NOLA, 80035 Nola, Italy

experimental setup was organized so as to cover flow ranges as wide as possible.

The main characteristics of the CI power unit used for performing the trials are listed in Table 1, and further details can be found in [18], [19]. The engine setup was chosen for closer operation to real-world use, as well as the availability of input signals that are representative for the intended application in automotive transportation. Apart from being closer to the actual use of EGR modules, this configuration was preferred with respect to a dedicated flow test bench, even though the latter would have ensured more thorough and precise evaluation of heat transfer characteristics.

TABLE I. ENGINE CHARACTERISTICS

Operating cycle	4 stroke, compression ignition
Cylinders	3
Bore x Stroke	75.0 mm x 77.6 mm
Displacement	1028 cm ³
Compression ratio	17.5:1
Rated power	15 kW @ 3600 rpm
Rated torque	60 Nm @ 2000 rpm
Fuel system	direct injection, common rail, 1400 bar maximum pressure
Air intake	naturally aspirated
Intake valves opening	13 deg bTDC
Intake valves closing	39 deg bTDC
Exhaust valves opening	38 deg bTDC
Exhaust valves closing	14 deg bTDC

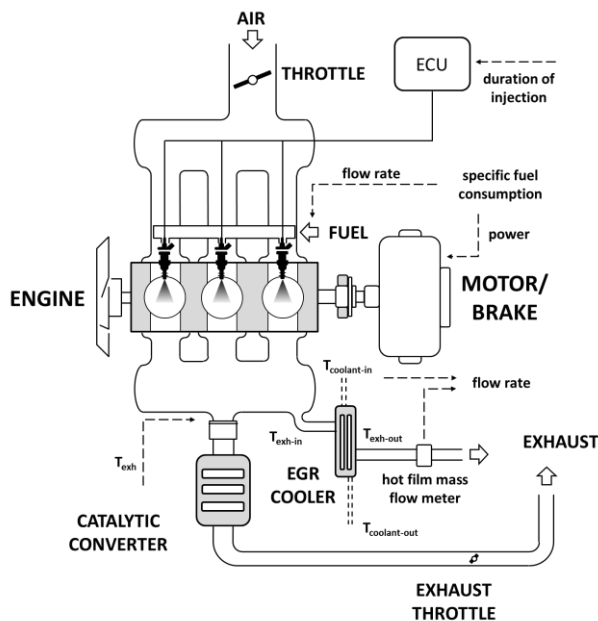


Figure 1. Schematic representation of the experimental setup

The EGR module was fitted at the exhaust of the engine (Figure 1), without any actual gas recirculation. This allowed a hot film mass flow meter to be used for measuring the entire flow of gas through the EGR valve. It was made possible by completely closing the exhaust throttle, and ensured stable

engine operation, even if exhaust backpressure was created. The setup also ensured redundant feedback of the actual flow, based on the readings of the engine's control unit air flow meter and injected quantity, similar to the aforementioned approach used for applying virtual sensors. With this configuration, a wide range of exhaust gas flow could be investigated, beyond the actual recirculation capabilities of the aspirated engine. A relatively large interval of pressure drop upstream-downstream of the valve could also be tested.

To get an idea of the actual EGR flow, an overall interval was established by using the results of a GT-Power [20] model of the commercial engines that employ the investigated module. A 'most frequent' use range was defined, based on the generic recirculation map previously mentioned; for example, it sets the highest rate of recirculation close to 40%, at engine speeds around 1600 rpm and low load, below 3 bar brake mean effective pressure (BMEP). In these conditions the air flow for the 1.2 liters engine is around 34 kg/h and over 20 kg/h exhaust gas flow into the intake manifold. The actual flow through the aspirated engine is over 90 kg/h at rated power, thus ensuring an ample margin for testing the EGR module in the considered configuration.

The main idea behind setting the operating conditions of the engine was to cover a wide range of recirculated exhaust gas flow, temperature and composition. For this reason, crankshaft rotational velocity was varied from 1500 to 3000 rpm, and relative air-fuel ratio was set in a range between 1.6 and 7. Engine output varied from 1 to 13 kW and resulting exhaust gas temperature was in a range from below 200 °C and up to maximum values close to 450 °C. Backpressure was maintained at values below 500 mbar, given that the aforementioned conditions of most frequent EGR use feature reduced boost. As an effort to ensure good repeatability, the power unit was allowed to reach rated coolant temperature during all trials; for each acquisition engine settings were kept constant, and data was recorded during a plateau-like temperature curves, therefore with steady-state thermal regime of the EGR module.

Measurements included gas and coolant flow values, as well as upstream-downstream temperature evaluations. All the instruments were chosen by considering the state-of-the-art for automotive sensors, thus completely compatible with the accuracies that can be expected during real-world operation [21]. Flow was determined with an ultrasonic volumetric meter that featured full scale values up to 25 liters/min and an accuracy of ±3% [22] for the liquid circuit and a hot film mass flow meter with readings up to 1000 kg/h [23]. Temperature measurements were performed with an accuracy of ±0.5 °C plus 0.2% of the measured value, by using K type thermocouples.

Two different parameters were calculated for evaluating heat transfer performance, i.e. effectiveness (η_{energy}) and efficiency (η_{temp}), by using equations (1) and (2) respectively,

$$\eta_{energy} = [dm_{gas} \cdot c_{p_{gas}} \cdot (T_{gas-in} - T_{gas-out})] / [dm_{liq} \cdot c_{liq} \cdot (T_{liq-out} - T_{liq-in})] \quad (1)$$

$$\eta_{temp} = (T_{gas-in} - T_{gas-out}) / (T_{gas-in} - T_{liq-in}) \quad (2)$$

where dm_{gas}/dm_{liq} is the flow of gas/liquid through the module measured in kg/s, c_{pgas}/c_{pliq} specific heat of exhaust gas/coolant liquid at constant pressure in J/kg K, $T_{gas-in/out}/T_{liq-in/out}$ gas/liquid temperatures measured in K, upstream/downstream of the module. The first parameter (i.e. effectiveness, basically an expression of the first law of thermodynamics [24]) can provide more information on the possible reasons of eventual changes observed in the performance of EGR modules. On the other hand, it requires flow measurements, which are much more difficult to implement. The second parameter (efficiency, calculated in a simplified version of the NTU method [25]) features easier integration.

For the more detailed analysis of heat exchange parameters, non-dimensional Nu , Re and Pr numbers were calculated using equations (3), (4) and (5),

$$Nu = h_{gas} \cdot d_{tube} / k_{gas} \quad (3)$$

$$Re = w_{gas} \cdot \rho_{gas} \cdot d_{tube} / \mu_{gas} \quad (4)$$

$$Pr = c_{pgas} \cdot \mu_{gas} / k_{gas} \quad (5)$$

where h_{gas} is the convective heat transfer coefficient calculated as $h_{gas} = dm_{gas} \cdot c_{pgas} / (n_{tubes} \cdot \pi \cdot d_{tube} \cdot l_{tube})$ and measured in $W/m^2 K$, n_{tubes} taken as 18 to mimic the geometry of the EGR module, d_{tube} diameter and l_{tube} is the length of each tube in m, k_{gas} thermal conductivity in $W/m K$, w_{gas} average gas velocity in m/s, ρ_{gas} density in kg/m^3 and μ_{gas} dynamic viscosity in Pa s. Only the gas side was investigated, as it is more prone to deterioration of heat transfer performance.

For comparison with the literature, Nu numbers were also calculated using equations (6) and (7) [24] for the laminar regime ($Re < 2300$),

$$Nu = 3.66 + (0.065 \cdot d_{tube} / l_{tube} \cdot Re \cdot Pr) / [1 + 0.04 \cdot (d_{tube} / l_{tube} \cdot Re \cdot Pr)^{2/3}] \quad (6)$$

$$Nu = 1.86 \cdot (Re \cdot Pr \cdot d_{tube} / l_{tube})^{1/3} \cdot (\mu_{bulk} / \mu_{surface})^{0.14} \quad (7)$$

with viscosity μ determined in bulk fluid conditions, as well as at the surface of the tube to account for temperature differences in the boundary layer. For all other equations average fluid temperature was used (i.e. $(T_{in} + T_{out}) / 2$).

Equations (8) [24] and (9) [26] were used for the transition regime ($2300 < Re < 10000$),

$$Nu = 0.125 \cdot f \cdot Re \cdot Pr^{1/3} \quad (8)$$

$$Nu = f/8 \cdot (Re - 1000) \cdot Pr / [1 + 1.27 \cdot (f/8)^{0.5} \cdot (Pr^{2/3} - 1)] \quad (9)$$

with friction factor f calculated as $f = [0.79 \cdot \ln(Re) - 1.64]^{-2}$ and no entry length or temperature corrections. These two choices were based on the assumption that the two effects are more likely to influence the laminar regime (e.g. the entry length for turbulent regimes is about 10 times less compared to laminar flow). Equation (8) features good accuracy for values of $Re > 10000$, while Gnielinski's correlation can be applied for ranges down to $Re > 3000$, even for ribbed tubes [27]. In the discussion section, reference will be made to results obtained with equation (6) as 'entry effect', (7) as 'temperature effect', (8) as 'Chilton-Colburn' and (9) as 'Gnielinski'.

III. Results and Discussion

As previously mentioned, the main idea behind organizing the experiments was to ensure a wide range of conditions that cover real-world application of the module. For example, the 55 kW engine features a value of 20 kg/h recirculated gas used most frequently, while the 77 kW one will obviously employ higher rates. Figure 2 shows the gas and coolant flow values that were tested during the experiments. As expected, there is no direct correlation between the two categories, meaning that liquid flow is mainly driven by engine speed values (the coolant pump was directly linked to the crankshaft) and opening of the thermostat valve, while gas flow was influenced by the volumetric stream through the engine (relatively well correlated to engine speed) and opening of the EGR valve. In fact, rotational velocity of the crankshaft is the common factor of influence for the two fluids.

Evidently, higher gas flow was obtained as the EGR valve was opened (i.e. at the same engine speed setting), with four different stages, at 25, 50, 75 and 100%. It should be noted that the actual valve lift features an exponential trend with respect to the four percentages (e.g. for 25% lift was around 0.5 mm out of a maximum of almost 7.5 mm, while at 50% lift was roughly 2 mm). An interesting observation is that at the 2000 rpm setting, gas and coolant flow seem to feature the same increasing trend from 25% to 75%, suggesting that the effect of additional load of EGR cooling results in increased opening of the thermostat. Of course, the reverting trend of coolant flow observed for 100% EGR opening emphasizes the complexity of heat fluxes in the coolant system (e.g. the engine featured a liquid-liquid heat exchanger for dissipating heat).

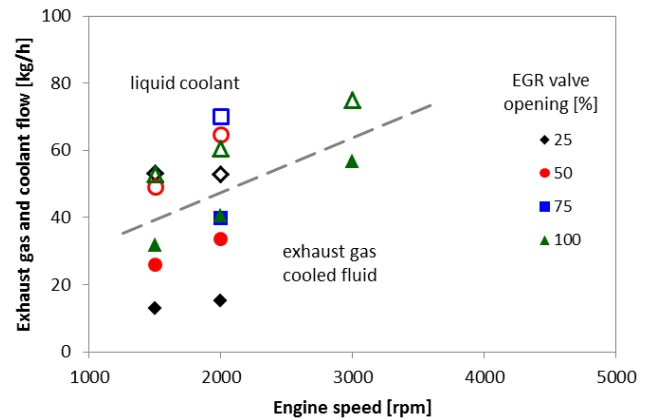


Figure 2. Flow values on the gas (solid symbols) and liquid (hollow symbols) sides

For the 2000 rpm condition output power was 10 kW; therefore a load of roughly 10 kW engine cooling can be expected. This needs to be compared to the heat flux transferred from the EGR module of around 2 kW. Even upstream-downstream temperatures were in a plateau regime during measurements, inertia in the aforementioned complex cooling system could have resulted in the observed changes in

the trend. This assertion is further emphasized by the quasi-constant liquid flow value at 1500 rpm.

As expected, exhaust gas temperature values upstream of the EGR module were higher as engine speed was increased (Figure 3). Temperature in-out differences ranged from 150 to 250 °C. One common trend was that this differences was lower as the EGR valve was opened. This is particularly evident for the 2000 rpm case, that featured four opening settings (evidently gas flow increased when switching from 25 to 50, 75 and 100%). An interesting observation is that increased engine speed featured more consistent temperature drop, for the same EGR valve setting. Given its higher specific heat, the liquid featured much more contained temperature differences. The largest modification was over 15 °C and the lowest below 4 °C. Evidently, larger mass flow and density effects also contribute to these reduced variations. As for the exhaust gas stream, higher coolant temperatures were recorded at increased engine speed. This trend was common for all EGR valve opening settings.

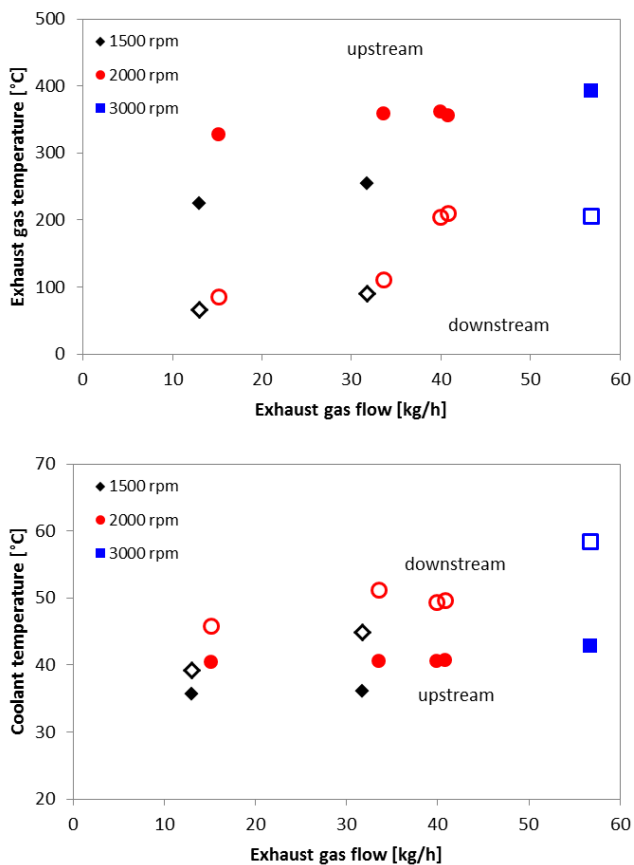


Figure 3. Gas (top) and coolant (bottom) temperature upstream (solid symbols) and downstream (hollow symbols) of the EGR module

The largest pressure difference was recorded at the minimum EGR valve opening (i.e. 25% setting), at 2000 rpm (Figure 4; please note that the values are gauge pressure). The effect of engine speed is evident when looking at the same valve opening; for the 25% case, gas flow increased at higher engine speed (over 15 kg/h for 2000 rpm compared to around

13 kg/h for the setting of 1500 rpm), associated with larger upstream-downstream pressure difference.

Obviously, the highest pressure difference at 100% valve opening was recorded at 3000 rpm (over 50 mbar). These trends at varying engine speed and EGR valve positions suggest that the most significant influence on pressure drop values was exerted by the flow past the valve rather than within the heat exchanger. This was to be expected, given the fact that the minimum flow area is given by the valve; it also emphasized the fact that when considering the numerical model, heat transfer in this region cannot be neglected, especially at partial openings.

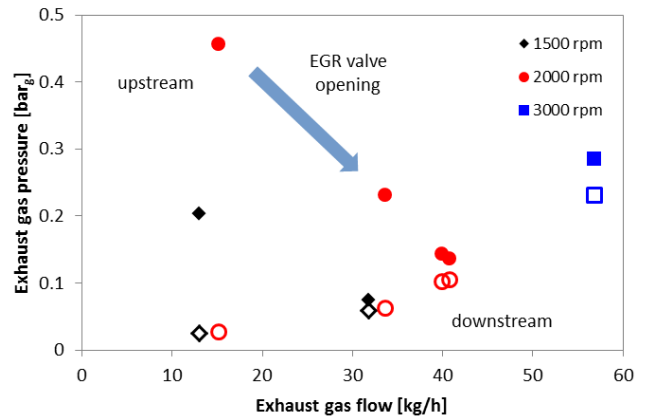


Figure 4. Gas pressure upstream (solid symbols) and downstream (hollow symbols) of the EGR module

Figure 5 shows efficiency values calculated using equation (1) for the effectiveness (labeled as energy efficiency) and equation (2) for the efficiency (the simplified NTU method). As mentioned in the previous section, the first parameter contains more information on what causes changes in the calculated parameter, while the second one only gives an idea on how efficient the heat exchanger is. Evidently, the latter requires only temperature measurements, possibly an enormous advantage with respect to straight forward applications and reduced costs. Nonetheless, one of the most important conclusions that can be drawn from the data shown in Figure 5 is that both methods deliver completely comparable results. Also, the peak effectiveness/efficiency values of over 80% are in line with values usually found in the literature for EGR modules [28]. As an overall trend, both parameters showed decreasing values as gas flow increased. This was more evident for the efficiency, while the effectiveness featured an initial increase as gas flow augmented and after a peak value of over 88% around 35 kg/h. Data dispersion was higher for effectiveness, while temperature only based efficiency showed narrower variations around a parabolic curve; the two points at 2000 rpm at 75 and 100% EGR valve opening make an exception in this sense. No clear conclusion could be drawn on why these conditions featured such low efficiency, especially as the point at 3000 rpm seems to confirm the aforementioned trend rather than suggesting significant effects of gas flow over a certain threshold.

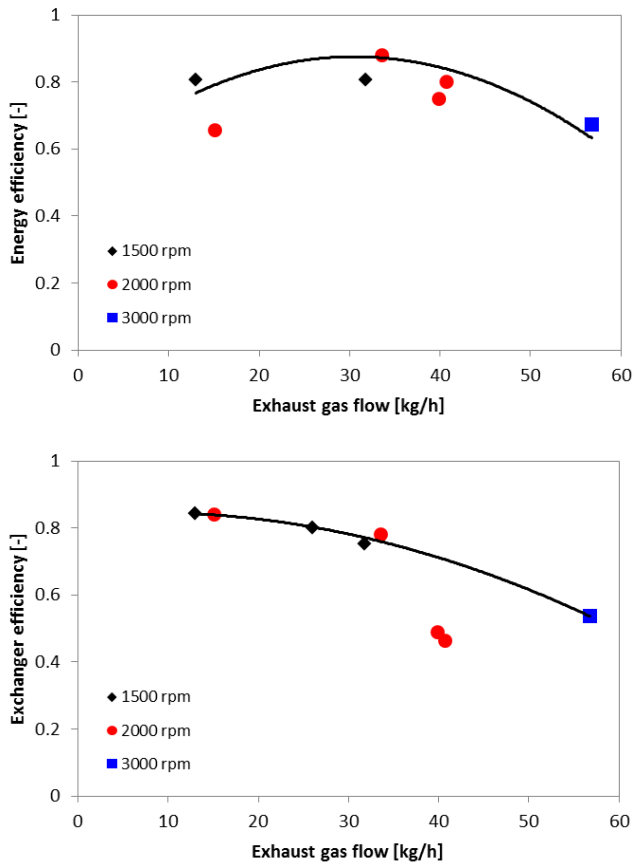


Figure 5. Effectiveness (top) and efficiency (bottom) calculated in the studied exhaust gas flow range

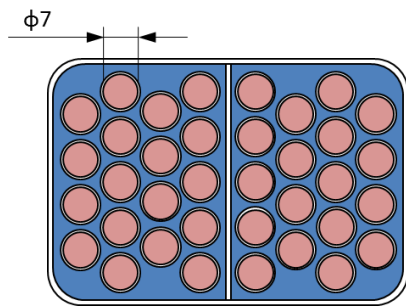


Figure 6. Heat exchanger inner geometry

As Figure 6 shows, the heat exchanger featured a symmetric cross-section, with a once-through configuration on each side, with gas flow inside and coolant flow outside the 18 tubes 7 mm in diameter. This resulted in 6.93 cm^2 flow section on the gas side. For the coolant side, the area of counter-parallel flow is 32.02 cm^2 and 11.55 cm^2 for cross-flow (with respect to the gas side). A more detailed analysis was performed with respect to the heat transfer coefficient (i.e. parameter h_{gas} used in equation (3), calculated based on the measured data). These experimental values were used for calculating Nu , Re and Pr numbers, using equations (3), (4) and (5) respectively. Figure 7 shows the experimental results,

as well as the values obtained by applying the correlations listed as equations (6), (7), (8) and (9).

As an overall observation, both equations for the laminar regime were close to the measurements, with the entry effect showing under-prediction, while the temperature effect relation slightly overshooting the experimental data. In the transition regime Gnielinski's correlation was closer to the current study; the Chilton-Colburn relation tends to overshoot the data. This was somewhat expected, given that equation (8) was developed for the turbulent regime (i.e. $Re > 10000$). Nonetheless, overall the correlations seem to be relatively accurate at predicting convective heat transfer coefficient values throughout the investigated flow range.

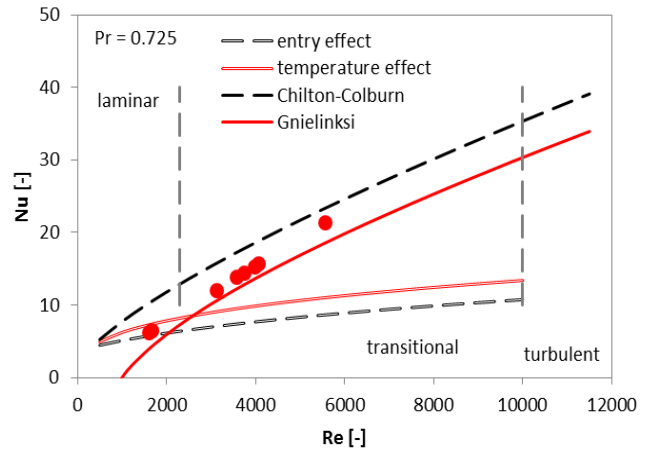


Figure 7. Correlation between Nu and Re numbers; data from the current experiment are represented with points, laminar equations are illustrated with double lines, while transitional-turbulent correlations with solid lines

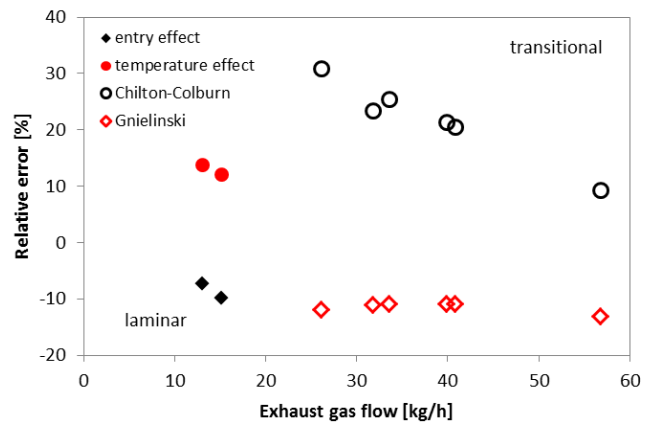


Figure 8. Relative error of empirical correlations from the literature with respect to heat transfer coefficient calculated based on experimental data

This is further emphasized by the relative error (calculated as $error = (Nu_{correlation} - Nu_{exp}) / Nu_{exp}$) shown in Figure 8. The values of this parameter in the laminar side of the graph show an interval of over $\pm 10\%$, which can be considered as acceptable. In the transitional part, maximum error levels were slightly over 30%, directly comparable with the stated

accuracy of equation (8) of around 25%. Gnielinski's correlation showed even better predictive capacity, with an error level close to the stated one of around 10%.

iv. Conclusion

An experimental campaign was designed and implemented for characterizing flow and heat transfer characteristics of an automotive cooled EGR module. The goal was to identify the route for building a model for hardware in the loop applications, with the end objective of developing a sensor for continuous efficiency evaluation of such components.

Overall efficiency values were found to be within the expected range for heat exchangers, with peak values close to 90%. The efficiency based on temperature measurements only was identified as the most convenient monitoring parameter, with easier integration within the sensor at reduced cost.

Convective heat transfer correlations with an empirical basis were found to feature good accuracy, close to 10% as the best obtained results, throughout the investigated flow range. Therefore, they be used without further calibration for developing the specific sub-models.

Acknowledgment

This work was financially supported in the VEDO project by the European Union and Campania Region of Italy, through the POR Campania FESR (European Regional Development Fund, original title in Italian) 2014-2020 program. The contribution of Carlo Rossi and Bruno Sgammato in the experimental activities is also gratefully acknowledged.

References

- [1] K. Morganti, M. Al-Abdullah, A. Alzubail, G. Kalghatgi, Y. Viollet, R. Head, A. Khan, A. Abdul-Manan, "Synergistic engine-fuel technologies for light-duty vehicles: Fuel economy and Greenhouse Gas Emissions," *Appl. Energy*, vol. 208, pp. 1538-1561, 2017, doi:10.1016/j.apenergy.2017.08.213.
- [2] G. Kalghatgi, "Is it really the end of internal combustion engines and petroleum in transport?," *Appl. Energy*, vol. 225, pp. 965-974, 2018, doi: 10.1016/j.apenergy.2018.05.076.
- [3] C.D. Rakopoulos, D.C. Rakopoulos, G.M., Kosmadakis, R.G., Papagiannakis, "Experimental comparative assessment of butanol or ethanol diesel-fuel extenders impact on combustion features, cyclic irregularity, and regulated emissions balance in heavy-duty diesel engine," *Energy*, vol. 174, pp. 1145-1157, 2019, doi: 10.1016/j.energy.2019.03.063.
- [4] J. Benajes, A. García, J. Monsalve-Serrano, S. Martínez-Boggio, "Emissions reduction from passenger cars with RCCI plug-in hybrid electric vehicle technology," *Appl. Therm. Eng.*, vol. 164, 114430, 2020, doi: 10.1016/j.applthermaleng.2019.114430.
- [5] M. Parravicini, C. Barro, K. Boulouchos, "Compensation for the differences in LHV of diesel-OME blends by using injector nozzles with different number of holes: Emissions and combustion," *Fuel*, vol. 259, 116166, 2020, doi: 10.1016/j.fuel.2019.116166.
- [6] F. Liu, J. Pfeiffer, "Estimation Algorithms for Low Pressure Cooled EGR in Spark-Ignition Engines," *SAE Int. J. Engines*, vol. 8, pp. 1652-1659, 2015, doi: 10.4271/2015-01-1620.
- [7] V. Macián, V. Bermúdez, D. Villalta, L. Soto, "Effects of low-pressure EGR on gaseous emissions and particle size distribution from a dual-mode dual-fuel (DMDF) concept in a medium-duty engine," *Appl. Therm. Eng.*, vol. 163, 114245, 2019, doi: 10.1016/j.applthermaleng.2019.114245.
- [8] R. Zhan, S. Eakle, J. Miller, J. Anthony, "EGR System Fouling Control," *SAE Int. J. Engines*, vol. 1, pp. 59-64, 2009, doi: 10.4271/2008-01-0066.
- [9] J. Hoard, M. Abarham, D., Styles, J., Giuliano, et al., "Diesel EGR Cooler Fouling," *SAE Int. J. Engines*, vol. 1, pp. 1234-1250, 2009, doi: 10.4271/2008-01-2475.
- [10] S. Park, K.S. Lee, J. Park, "Parametric Study on EGR Cooler Fouling Mechanism Using Model Gas and Light-Duty Diesel Engine Exhaust Gas," *Energies*, vol. 11, 3161, doi: 10.3390/en11113161.
- [11] C. Sluder, J. Storey, M. Lance, "Effectiveness Stabilization and Plugging in EGR Cooler Fouling," *SAE Technical Paper 2014-01-0640*, 2014, doi: 10.4271/2014-01-0640.
- [12] D. Pachner, J. Beran, J. Tigelaar, "Uncertainty Analysis of a Virtual Turbo Speed Sensor," *SAE Technical Paper 2016-01-0096*, 2016, doi:10.4271/2016-01-0096.
- [13] S. Lee, Y. Lee, K. Han, K. Lee, et al., "Virtual NOx sensor for Transient Operation in Light-Duty Diesel Engine," *SAE Technical Paper 2016-01-0561*, 2016, doi: 10.4271/2016-01-0561.
- [14] D. Pachner, J. Beran, "Comparison of Sensor Sets for Real-Time EGR Flow Estimation," *SAE Technical Paper 2016-01-1064*, 2016, doi: 10.4271/2016-01-1064.
- [15] S. Tsironas, O. Stenlaas, M. Apell, A. Cronhjort, "Heavy-Duty Engine Intake Manifold Pressure Virtual Sensor," *SAE Technical Paper 2019-01-1170*, 2019, doi: 10.4271/2019-01-1170.
- [16] A. Zschutschke, J. Neumann, D. Linse, C. Hasse, "A systematic study on the applicability and limits of detailed chemistry based NOx models for simulations of the entire engine operating map of spark-ignition engines," *Appl. Therm. Eng.*, vol. 98, pp. 910-923, 2016, doi:10.1016/j.applthermaleng.2015.12.093.
- [17] E. Tosun, K. Aydin, S.S. Merola, A. Irimescu, "Estimation of operational parameters for a direct injection turbocharged spark ignition engine by using regression analysis and artificial neural network," *Therm. Sci.*, vol. 21, pp. 401-412, 2017, doi:0.2298/TSCI160302151T.
- [18] A. Magno, E. Mancaruso, B.M. Vaglieco, "Analysis of combustion phenomena and pollutant formation in a small compression ignition engine fuelled with blended and pure rapeseed methyl ester," *Fuel*, vol. 106, pp. 618-630, 2016, doi: 10.1016/j.energy.2016.03.106.
- [19] S. Di Iorio, A. Magno, E. Mancaruso, B.M. Vaglieco, "Analysis of the effects of diesel/methane dual fuel combustion on nitrogen oxides and particle formation through optical investigation in a real engine," *Fuel Proc. Technol.*, vol. 159, pp. 200-210, 2017, doi: 10.1016/j.fuproc.2017.01.009.
- [20] *** Gamma Technologies, *GT-SUITE Flow Theory Manual Version 7.4*, 2013.
- [21] J.B. Heywood, *Internal Combustion Engine Fundamentals*, New York: McGraw Hill, 1988.
- [22] *** Cynergy³ Components Ultrasonic Flow Meter UF25B, Technical data, 2018.
- [23] *** Bosch Hot-film air-mass meter, Type HFM 5 Technical data, 2012.
- [24] Y.A. Çengel, A.J. Ghajar, *Heat and Mass Transfer: Fundamentals and Applications*, 4th ed., Chapter 8, McGraw-Hill, New York, United States of America, 2010.
- [25] F.P. Incropera, D.P. Dewitt, T.L. Bergman, A.S. Lavine, *Fundamentals of heat and mass transfer*, 6th edition, Chapter 11, John Wiley & Sons, 2007.
- [26] V. Gnielinski, "New equations for heat and mass transfer in turbulent pipe and channel flow," *Int. Chem. Eng.*, vol. 16, pp. 359-368, 1976.
- [27] W.T. Ji, D.C. Zhang, Y.L. He, W.Q. Tao, "Prediction of fully developed turbulent heat transfer of internal helically ribbed tubes – An extension of Gnielinski equation," *Int. J. Heat Mass Transfer*, vol. 55, pp. 1375-1384, 2012, doi: 10.1016/j.ijheatmasstransfer.2011.08.028.
- [28] J. Lee, K. Min, "A study of the fouling characteristics of EGR coolers in diesel engines," *J. Mech. Sci. Technol.*, vol. 28, pp. 3395-3401, 2014, doi: 10.1007/s12206-014-0752-8.